The new centrifuge high-speed pellet injector for ASDEX Upgrade

P.T. Lang, C. Andelfinger, W. Beck, E. Buchelt,
K. Büchl, P. Cierpka, H. Kollotzek, R.S. Lang,
G. Prausner, F.X. Söldner, M. Ulrich and G. Weber

IPP 1/274 April 1993

MAX-PLANCK-INSTITUT FÜR PLASMAPHYSIK

8046 GARCHING BEI MÜNCHEN

MAX-PLANCK-INSTITUT FÜR PLASMAPHYSIK

GARCHING BEI MÜNCHEN

The new centrifuge high-speed pellet injector for ASDEX Upgrade

P.T. Lang, C. Andelfinger, W. Beck, E. Buchelt,
K. Büchl, P. Cierpka, H. Kollotzek, R.S. Lang,
G. Prausner, F.X. Söldner, M. Ulrich and G. Weber

IPP 1/274 April 1993

Die nachstehende Arbeit wurde im Rahmen des Vertrages zwischen dem Max-Planck-Institut für Plasmaphysik und der Europäischen Atomgemeinschaft über die Zusammenarbeit auf dem Gebiete der Plasmaphysik durchgeführt.

The new centrifuge high-speed pellet injector for ASDEX Upgrade

P.T. Lang, C. Andelfinger, W. Beck, E. Buchelt,
K. Büchl, P. Cierpka, H. Kollotzek, R.S. Lang,
G. Prausner, F.X. Söldner, M. Ulrich and G. Weber

Max-Planck-Institut für Plasmaphysik
EURATOM Association
85748 Garching bei München, Germany

ABSTRACT

We report on the new pellet injection system for refuelling the ASDEX Upgrade tokamak with cubic H_2 or D_2 pellets having alternative side lengths of 1.5, 1.75 and 2.0 mm and optional Ne doping. The system delivers series of about one hundred pellets at a maximum repetition rate of more than 40 Hz. The pellets are accelerated by means of a centrifuge with an optimized straight acceleration arm. This configuration minimizes the compulsive force acting on the pellet during the acceleration process. Since this also minimizes stresses inside the pellet, high velocities - a maximum of 1211 m/s being achieved - are possible without destroying the hydrogen cubes. A special pellet feed-in technique based on a static stop cylinder interrupting the acceleration path successfully reduced the horizontal scattering angle to values of less than ± 4 degrees. Thus, a high efficiency - with more than 90 % of the pellets arriving within the acceptance angle - was achieved without using a guide tube. The whole system was found to work very reliably and reproducibly during the whole test operation period, covering about 10^5 pellet shots. The new centrifuge, now integrated into the ASDEX Upgrade setup, has proved to be a reliable unit even for long operation periods thus affording the possibility of quasicontinuous particle refuelling throughout a plasma discharge in ASDEX Upgrade.

Table of Contents

1. INTRODUCTION

One of the main tasks still to be solved before successful operation of a thermonuclear fusion reactor is how to refuel the active medium. Most of the scenarios recommended for a future tokamak reactor suggest DT fusion where the plasma is continuously fuelled with the deuterium and tritium, the latter bred from the Li blanket [1]. There are two main methods of refuelling the plasma: gas puffing and injection of frozen pellets. The major advantage of pellet injection over gas puffing is that particles are deposited behind the separatrix in a region where closed magnetic surfaces allow a higher fuelling efficiency. Moreover, transport phenomena inside the plasma cause peaking of the electron density profile, as confirmed by many experiments in ASDEX [2]. Another benefit of the injective fuelling method is that exhaust of the fuel ash can be better controlled by flushing out the He atoms by friction with the hydrogen atoms in the boundary layers of the plasma when refuelling occurs mainly in this region [3].

To achieve pellets of adequate mass and velocity, two kinds of accelerators are now in use, namely gas guns and centrifuges. An up-to-date overview of results achieved by these methods is given in Ref. [4]. With gas guns it is possible to accelerate pellets to very high velocities (up to 3800 m/s has been reported [5]); however, the total number of pellets available and the repetition frequency are limited (the latter to 6 Hz) and great technical effort is necessary to prevent the propulsion gas from entering the plasma required by the pneumatic gun. Centrifuge accelerators are able to deliver series comprising a greater number of pellets with appropriate masses for refuelling; the maximum velocities available, however, are less than for gas guns (up to 800 m/s for Doublet-III [6]). This paper reports on a newly developed centrifuge system for accelerating large series of pellets with appropriate masses at a high repetiton rate to velocities which, to our knowledge, have not yet been achieved with such systems.

2. THE CENTRIFUGE HIGH-SPEED PELLET INJECTION SYSTEM

The main parts of the system are the gas supply system, the extrusion and storage cryostats, the centrifuge itself, the computerized control system and the diagnostics unit. First an appropriate amount of the gaseous pellet material is prepared inside the gas supply system and then injected into the extrusion cryostat, where it is frozen. Next the material is extruded into the storage cryostat, where the fuel rod is kept until required. When a request signal arrives, a cubic pellet is cut from the rod and fed into the centre part of the centrifuge. There, the radial acceleration is first stopped by a static stop cylinder, where the pellets slide along azimuthally to an exit window, through which the pellets enter the straight rotating arm and are accelerated to their final speed. They leave the arm at an angle of 45 degrees and then enter the diagnostic unit. Here their velocities, vertical and horizontal scattering angles and shapes are analyzed. Detailed descriptions of all essential items are given in the following.

2.1 Gas supply system

The gas supply system stores bottles containing high-purity charges of different gases: He, H_2, D_2 and Ne. The He gas ventilates the complete system, and the high-purity (99.999 %) H_2 or D_2 serves for fuelling the extrusion cryostat. Moreover, it offers the possibility of admixing small amounts of Ne to the fuelling gas to allow the investigation of transport of impurities in the target plasma [7].

2.2 The cryostat system: pellet production

The cryostat system comprises two parallel systems, one for the extrusion cryostat and the other for the storage cryostat. Their basic temperature control is based on the pressure difference over the cryostats in the liquid-helium circuit. The helium flux is controlled by pressure and flux measurements; the mean consumption is about 5 l/h per cryostat. Changes in the temperature of the extrusion cryostat are produced by controlled electric heating. Extrusion is performed with a hydraulic piston. All valves are controlled by electropneumatic valves in order to ensure galvanic separation of the different circuits. A sketch of the helium circuits is shown in Fig. 1. A combination of three double-acting pistons shifts the extrusion nozzle to 4 positions, namely for three pellet cross-sections and the closed position for fuelling the extrusion cryostat.

For pellet production, first the pellet material desired is frozen in the extrusion cryostat at a temperature of about 4 K. The solid fuel material is then conditioned by varying the temperature and pressure. By applying about 7 K for H_2 and 13 K for D_2 and a pressure of 300 to 400 bar the material is extruded through the nozzle, which determines the quadratic cross-section of the fuel rod produced. This 192 mm long rod is now stored at the appropriate temperature (4 K for H_2 and 6 K for D_2). The storage cryostat contains a separate channel for each different pellet size. The rigid fuel rod is pushed by a lever driven by a stepping motor through the exit of the storage cryostat. The number of steps determines the pellet length; the step size of 0.25 mm determines the fineness of the possible pellet length. Both, the extrusion nozzle and the storage cryostat can be moved pneumatically inside the vacuum system to select the pellet size. A schematic drawing of the cryostat system as it is mounted on the centrifuge is shown in Fig. 2.

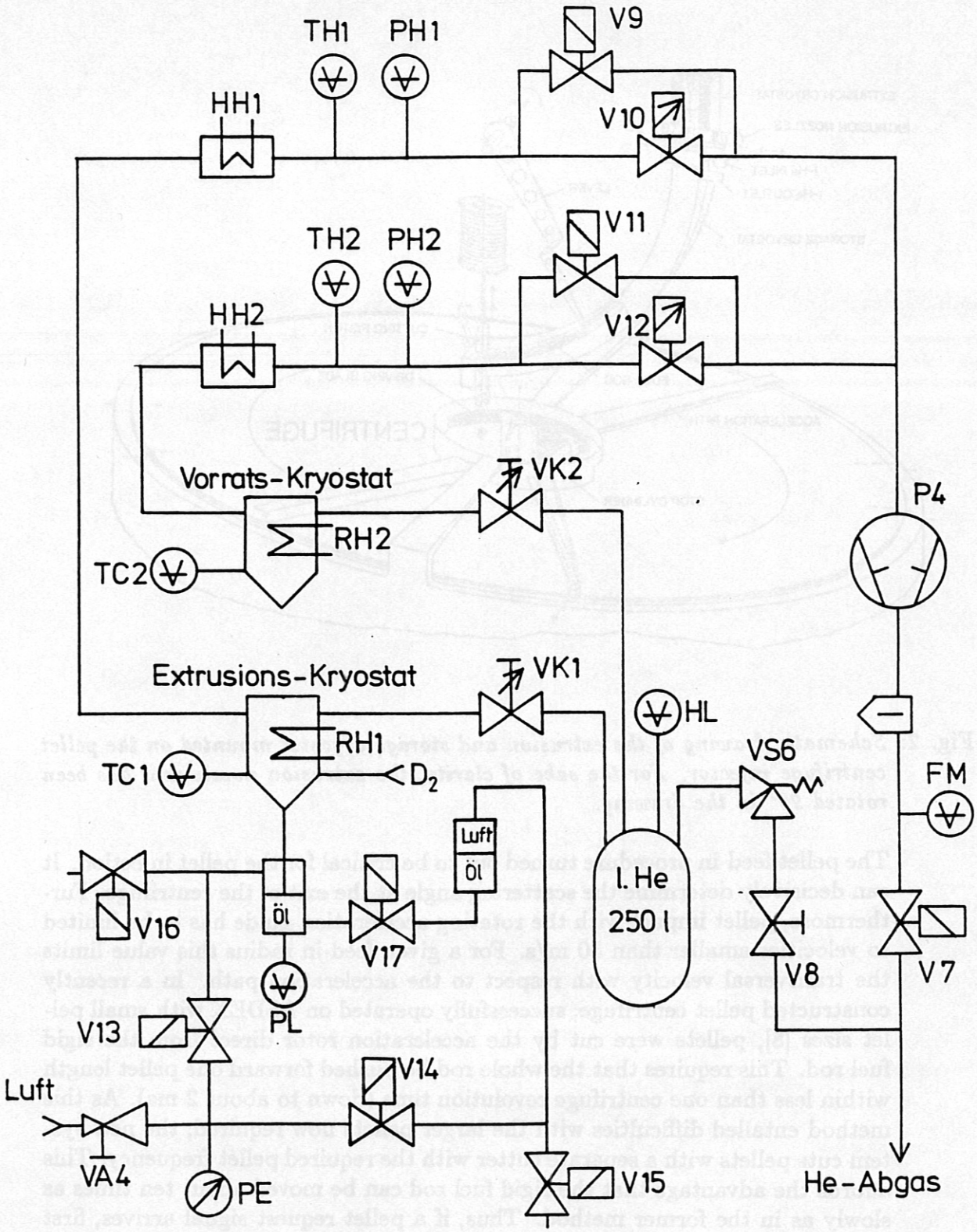

Fig. 1: *Circuits of the helium cooling system.*

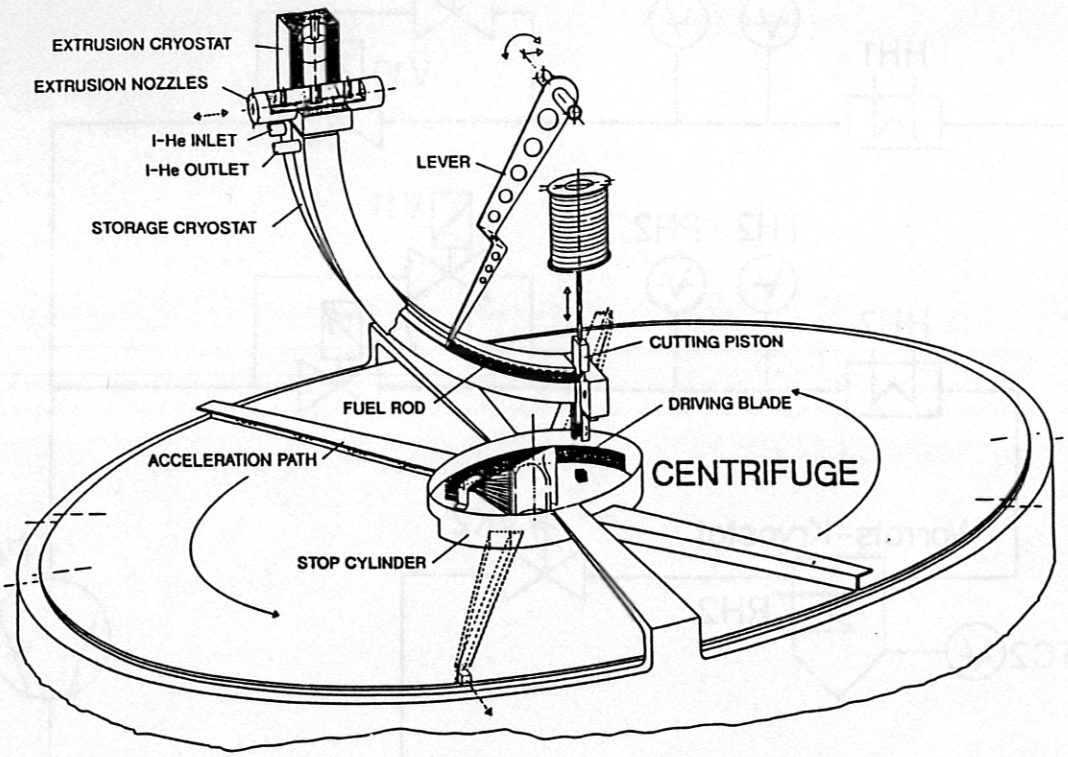

Fig. 2: *Schematic drawing of the extrusion and storage cryostat mounted on the pellet centrifuge injector. For the sake of clarity, the extrusion nozzle unit has been rotated 90° in the drawing.*

The pellet feed-in procedure turned out to be critical for the pellet injection. It can decisively determine the scattering angle at the exit of the centrifuge. Furthermore, pellet impact with the rotating acceleration guide has to be limited to velocities smaller than 50 m/s. For a given feed-in radius this value limits the transversal velocity with respect to the acceleration path. In a recently constructed pellet centrifuge, successfully operated on ASDEX with small pellet sizes [8], pellets were cut by the acceleration rotor direct from the rigid fuel rod. This requires that the whole rod be pushed forward one pellet length within less than one centrifuge revolution time (down to about 2 ms). As this method entailed difficulties with the larger pellets now required, the new system cuts pellets with a separate cutter with the required pellet frequency. This affords the advantage that the rigid fuel rod can be moved about ten times as slowly as in the former method. Thus, if a pellet request signal arrives, first the step motor pushes out part of the fuel rod to the length preselected. Then, the electronic control system brings the cutting knife into action with a time delay to synchronize the cutting to the centrifuge rotation in order to feed in the pellet at the correct time. The cutter itself moves perpendicularly to the pushing direction of the rod and accelerates the pellets to velocities of about 4 m/s. It is thus ensured that the pellets cover the distance of 15 mm straight down to the acceleration guide within one revolution of the centrifuge.

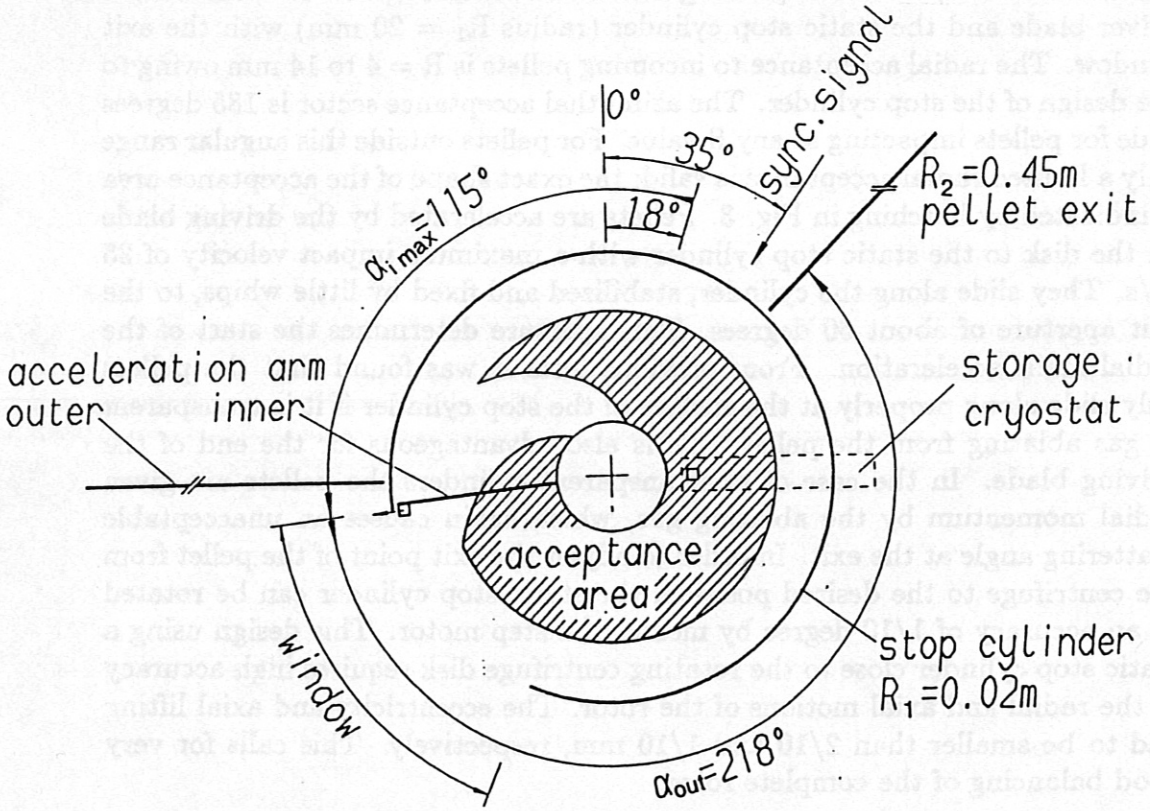

Fig. 3: *Diagram of pellet feed-in and acceleration procedure: The acceleration angles are independent of the centrifuge revolution frequency* $\alpha = (360/2\pi) * arccosh(R_2/R_1)$*: in our case the outer acceleration angle is 218° and the minimum and maximum inner acceleration angles are 47° and 115°, respectively. Acceleration therefore has to start at* $45° + 218° + 115° = 378° \equiv 18°$ *at the earliest. To cross the gap between the inner and outer acceleration arm, an angle of about 30° is necessary, which means that the window in the stop cylinder has to be larger than that. The actual width is 60°. A synchronization signal is given at 35°. After a delay* ΔT *depending on the centrifuge frequency pellets are cut at 90°, well inside the acceptance area of the central disk.*

2.3 Pellet acceleration

a) Inner driving blade and stop cylinder

The arrival position of the pellets strongly differs from shot to shot, which is most probably due to internal stresses in the fuel rod and sticking of the pellets to the cutter. This would cause a huge angular spread at the exit of the centrifuges if no further steps were taken to prevent this. The new method applied in our centrifuge to suppress this effect is to stop the radial movement of the pellet at a certain radius on the centrifuge disk and then start acceleration from a certain position. This way, all pellets have almost identical starting conditions for the acceleration process and thus leave the centrifuge on almost identical trajectories. The principal feature of the centrifuge, rotating

counterclockwise, for accomplishing this is shown in Fig. 3. It consists of a driver blade and the static stop cylinder (radius $R_1 = 20$ mm) with the exit window. The radial acceptance to incoming pellets is R = 4 to 14 mm owing to the design of the stop cylinder. The azimuthal acceptance sector is 185 degrees wide for pellets impacting at any R value. For pellets outside this angular range only a limited radial acceptance is valid; the exact shape of the acceptance area is indicated by hatching in Fig. 3. Pellets are accelerated by the driving blade on the disk to the static stop cylinder with a maximum impact velocity of 35 m/s. They slide along the cylinder, stabilized and fixed by little whips, to the exit aperture of about 60 degrees. This aperture determines the start of the radial main acceleration. From previous tests it was found that the pellets only slide along properly at the surface of the stop cylinder if it is transparent to gas ablating from the pellet; this is also advantageous for the end of the driving blade. In the case of nontransparent cylinders the pellets are given radial momentum by the ablating gas, which again causes an unacceptable scattering angle at the exit. In order to adjust the exit point of the pellet from the centrifuge to the desired position, the static stop cylinder can be rotated to an accuracy of 1/10 degree by means of a step motor. This design using a static stop cylinder close to the rotating centrifuge disk requires high accuracy of the radial and axial motions of the rotor. The eccentricity and axial lifting had to be smaller than 2/10 and 1/10 mm, respectively. This calls for very good balancing of the complete rotor.

b) Acceleration on the straight arm

When the pellets pass through the exit window and enter the straight outer acceleration arm, they undergo their actual acceleration process. In order to find out how this acceleration takes place, let the pellet be considered as a point mass m. For the equation of motion within an inertial system K Newton's law holds:

$$m\frac{d^2}{dt^2}\boldsymbol{r}(t) = \boldsymbol{F}(\boldsymbol{r},t), \tag{1}$$

where $\boldsymbol{r}(t)$ is the positon of the mass point and $\boldsymbol{F}(\boldsymbol{r},t)$ are the forces acting on the pellet. In the system $\boldsymbol{K}'$ rotating with the angular velocity ω around the z-axis, eq. (1) transforms to [9]

$$m\frac{d'^2}{dt^2}\boldsymbol{r}(t) = \boldsymbol{F}(\boldsymbol{r},t) - 2m\boldsymbol{\omega}\times\frac{d'}{dt}\boldsymbol{r} - m\boldsymbol{\omega}\times(\boldsymbol{\omega}\times\boldsymbol{r}) - \left(\frac{d'}{dt}\boldsymbol{\omega}\right)\times\boldsymbol{r}, \tag{2}$$

where the prime denotes the changes observed in $\boldsymbol{K}'$. If plane polar coordinates are used and counterclockwise rotation with constant angular velocity ($\omega = 2\pi f = const.$, with f the centrifugal revolution frequency) around the origin is assumed, eq. (2) becomes

$$m\frac{d'^2}{dt}\boldsymbol{r}(t) = \boldsymbol{F}(\boldsymbol{r},t) - 2m\boldsymbol{\omega}\times\boldsymbol{v}' + m\omega^2 r\hat{e}_r. \tag{3}$$

When acceleration takes place on a straight arm, compulsive forces occur and prevent v' from having components perpendicular to $\hat{e}_r$. Thus, the acceleration

is directed radially due to the centrifugal term obeying

$$m\frac{d^{2\prime}}{dt^2}r(t) = \boldsymbol{F}(r,t) + m\omega^2 r\hat{e}_r, \tag{4}$$

whereas compulsive forces act to compensate for the Coriolis force

$$F_c = 2m\omega v'. \tag{5}$$

In the absence of additional forces eq. (4) becomes the simple differential equation

$$\ddot{r} = \omega^2 r \tag{6}$$

with the solution

$$r(t) = Ae^{\omega t} + Be^{-\omega t}, \tag{7}$$

with A and B being determined by the starting conditions $r_o \equiv r(t=0)$ and $v_o \equiv v(t=0)$. In the case of an acceleration starting at r_1 with velocity $v_o = 0$ eq. (7) yields

$$\begin{aligned} r(t) &= \frac{r_1}{2}(e^{\omega t} + e^{-\omega t}) = r_1\ cosh(\omega t), \\ v(t) &= \frac{\omega r_1}{2}(e^{\omega t} - e^{-\omega t}) = r_1\ sinh(\omega t) \end{aligned} \tag{8}$$

By calculating the kinetic energy of the particle,

$$E_{kin} = \int_{r_1}^{r_2} m\omega^2 r\ dr = \frac{m\omega^2}{2}(r_2^2 - r_1^2), \tag{9}$$

the radial velocity v_r achieved by the pellet after acceleration from r_1 to r_2 is found to be

$$v_r = \omega r_2\sqrt{1 - \left(\frac{r_1}{r_2}\right)^2} \tag{10a}$$

or, in the case $r_1 \ll r_2$, approximately

$$v_r \approx \omega r_2\left(1 - \frac{1}{2}\left(\frac{r_1}{r_2}\right)^2\right). \tag{10b}$$

The velocity v_p of the pellet when leaving the acceleration arm at r_2, observed in the laboratory system $\boldsymbol{K}$, is then given by

$$v_p = \sqrt{v_r^2 + v_\omega^2}, \tag{11}$$

where $v_\omega = \omega r$ is the angular velocity of the pellet at r_2. Using eq. (10a), one obtains

$$v_p = \omega r_2\sqrt{2 - \left(\frac{r_1}{r_2}\right)^2} \tag{12a}$$

or, using (10b), approximately

$$v_p \approx \sqrt{2}\omega r_2 \left(1 - \frac{1}{4}\left(\frac{r_1}{r_2}\right)^2\right). \tag{12b}$$

The angle of the pellet with respect to the straight acceleration arm is

$$\alpha = arcctg\left(\frac{1}{\sqrt{1-\left(\frac{r_1}{r_2}\right)^2}}\right) \tag{13a}$$

or, for $r_2/r_1 \ll 1$, approximately

$$\alpha \approx \frac{\pi}{4} - \frac{1}{4}\left(\frac{r_1}{r_2}\right)^2. \tag{13b}$$

The acceleration angle φ can be calculated from the acceleration time T. Starting at r_1 at $t = 0$, the pellet reaches r_2 at the time T, and so it follows from eq. (13)that

$$r_2 = \frac{r_1}{2}\left(e^{\omega T} + e^{-\omega T}\right) = r_1 \; cosh(\omega T)$$

and hence

$$T = \frac{arccosh\frac{r_2}{r_1}}{\omega}. \tag{14}$$

During the time period T the acceleration arm passes through the acceleration angle

$$\varphi = \frac{360^o}{2\pi} arccosh\frac{r_2}{r_1}, \tag{15}$$

whose value is independent of the centrifuge revolution frequency.
Using $r_1 = 0.02$ m and $r_2 = 0.45$ m as realized in the centrifuge, one obtains a pellet velocity

$$v_p = 3.997[\mathrm{m}] * f[1/\mathrm{s}], \tag{16}$$

an exit angle α of 45.028 degrees and an acceleration angle φ of 218.077 degrees.

The survival of the pellets during acceleration is a critical point. In general, centrifugal and compulsive forces act on the pellet in accordance with the acceleration path.
In order to reduce compulsive forces on the pellet, one can use either a straight acceleration arm or a disk accelerator with an acceleration path of constant compulsive force and tangential pellet exit [10], both yielding minimum compulsive forces at a given pellet velocity. The stress-optimized disk accelerator, however, has the disadvantage of a larger inertia, higher loads acting on the bearings and, most important, a very high risk potential preventing its use for refuelling experiments at the pellet velocity range aimed at. We thus chose a straight acceleration arm. Owing to the compulsive force $F_C = 2\ m_p\ r\omega^2$

present here, it seems most favourable to keep the revolution frequency small and the radius large. Space requirements and the available rotor prescribed $R_2 = 0.45$ m and a maximum f of 300 Hz ($\omega = 1885$ 1/s), yielding a conservative value of $F_C = 3.2 * 10^6 * m_p$[N] for the compulsive force. For the cubic pellet shapes used the contact pressure is therefore up to 1.3 MPa. Though this is well above the maximum static yield stress of hydrogen at the temperatures used, the pellets were found to withstand even higher loads in previous pellet injection experiments on ASDEX. This behaviour was ascribed to the short acceleration time of less than a millisecond.

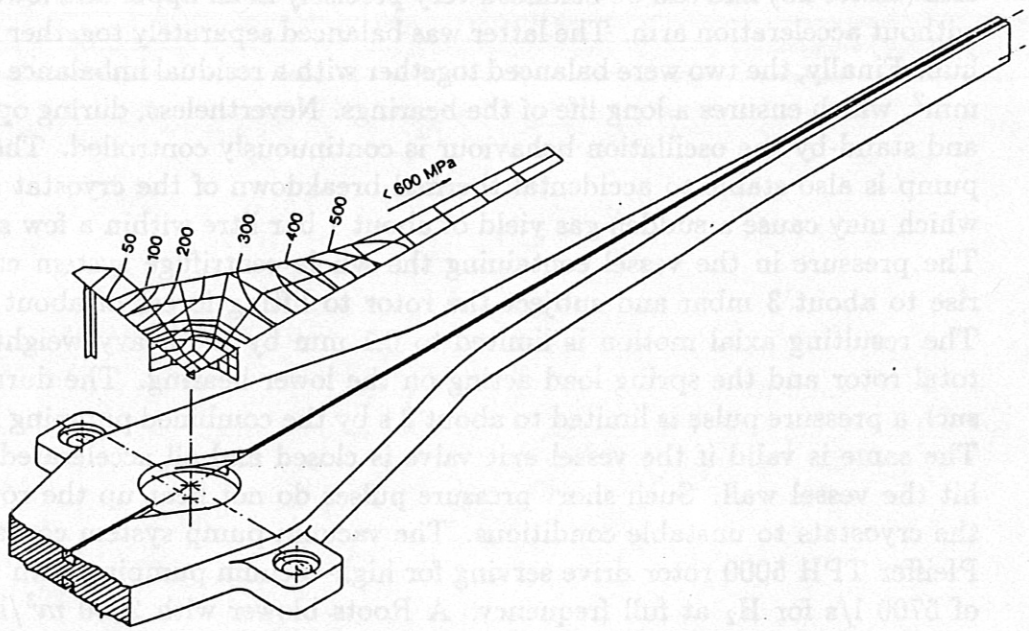

Fig. 4: *Outer acceleration arm and 1/4 model of the finite-element calculation with lines of constant stress indicated.*

For realization of the acceleration arm high-tech materials such as carbon fibre compounds seemed to be good candidates in view of their low mass and hence low risk. This choice, made in collaboration with two high-tech firms, was a failure, probably because fusibility and loss of resin resulted in large imbalance and destruction of the rotor arm. This setback was followed by the design of an optimized arm made of an alloy with well-known properties, namely TiAl6V4, with a tensile strength of $\sigma_{0.2} = 1160$ MPa. The variation in cross-section is such that the resulting stresses - according to the von Mises yield criterion [11] - will nowhere be larger than 600 MPa with 5 % overspeed. This was confirmed by a two-dimensional finite-element calculation, which also predicted a fatigue limit exceeding 10^7 load cycles for the operation conditions. Figure 4 shows part of the arm and a 1/4 model for the finite-element calculation. The cross-section ratio has to be $6 \geq Q_o/Q_1$, where Q_o is the cross-section of the arm at the rotation axis and Q_1 the cross-section of the linear part at the end of the arm. In reality, the cross-section is oversized. The manufacturing tolerance has to be less than 1/100 mm to ensure that the imbalance will

be reasonably limited. Special care was taken with the centring hub. The noncircularly symmetric elongation of the arm deforms the centring ring, which works like a spring without any hysteresis due to friction. Another important point confirmed by dynamic calculations is that all oscillation modes of the arm are always above the rotation frequency [12].

c) Driver pump and vacuum system
The drive selected for the centrifuge is a Pfeiffer TPH 5000 turbomolecular pump, which has several favourable features. The rotating part of this pump has a very large axial inertial moment compared with that of the acceleration arm (factor 20) and can be balanced very precisely in an upper and lower plane without acceleration arm. The latter was balanced separately together with its hub. Finally, the two were balanced together with a residual imbalance of 100 g mm^2, which ensures a long life of the bearings. Nevertheless, during operation and stand-by the oscillation behaviour is continuously controlled. The driver pump is also stable to accidental thermal breakdown of the cryostat system, which may cause a sudden gas yield of about 1 bar litre within a few seconds. The pressure in the vessel containing the whole centrifuge system can then rise to about 3 mbar and subject the rotor to lifting forces of about 100 N. The resulting axial motion is limited to 0.1 mm by the heavy weight of the total rotor and the spring load acting on the lower bearing. The duration of such a pressure pulse is limited to about 3 s by the combined pumping system. The same is valid if the vessel exit valve is closed and all accelerated pellets hit the vessel wall. Such short pressure pulses do not heat up the rotor and the cryostats to unstable conditions. The vacuum pump system contains the Pfeiffer TPH 5000 rotor drive serving for high-vacuum pumping with a speed of 5700 l/s for H_2 at full frequency. A Roots blower with 2000 m^3/h and a rotary vane pump with 120 m^3/h in series provide the backing vacuum.
To reduce stresses within the centrifuge system during operation, the load on the centrifuge upper bearing was measured for rotation frequencies of up to 300 Hz, and then four appropriate frequencies (60, 150, 230 and 300 Hz) were chosen for long-term operation. Full ventilation at full speed produces thermal expansion of the rotor axis of a few tenths of a millimetre. Ventilation of the vessel has therefore been restricted to a turbine frequency of less than 50 Hz.

2.4 Local control unit

System control and data acquisition are performed by a computer system consisting of a Siemens Simatic S5 and a COROS. These computers are PC-like, rugged, block-type, memory-programmed control units where the logical connections are valid as programs within the unit. This unit runs the whole process of fuel rod production and also supervises the synchronization and the appropriate delay of the cutting signal with respect to the current operation conditions. This way, any desired sequence of pellet injection times can be chosen up to the maximum repetition rate. Moreover, all relevant parameters measured within the apparatus, such as temperatures, pressures, currents, frequencies and the load on the centrifuge, are permanently controlled. In case of perturbation within the system or failure of part of the apparatus, the control unit brings the whole system to a standstill in an appropriate manner that avoids further damage.

2.5 Testbed diagnostics unit

In the testbed facilities the pellet passes through a number of different diagnostics when leaving the vessel's exit port in order to determine some of the pellet's most important properties. First, it passes through a linear array of 9 light barriers, where the horizontal scattering angle is measured to an accuracy of about 0.5 degrees. As the total length of this detector array at its given distance from the centre of the centrifuge is equivalent to an angle of ± 4 degrees, i.e. the acceptance angle on ASDEX Upgrade, the sum of all signals indicates the total efficiency of the pellets available for plasma refuelling. A trigger signal delivered by this detector array when traversed by a pellet was used as the main trigger signal for the further diagnostics; this signal also serves to indicate the arrival of a pellet in the plasma when refuelling experiments are performed.

Next, a picture is taken of the pellet to check whether it is subject to deformation or even destruction. To avoid movement blur caused by the high velocity of the pellet, a short infrared (ir) laser pulse emitted from a GaAs laser diode (wavelength 904 nm, pulse duration 70 ns FWHM, pulse power 20 W) was applied for illumination. Observation is made with an ir-sensitive CCD camera, the current picture being captured by an electronic freezer and than recorded on video tape. Since the video system stores one picture every 20 ms, it is possible to document each pellet even at the highest possible pellet repetition rates (43 Hz). To determine the pellet velocity, a time-of-flight measurement is made. Two light barriers, 50 cm apart, generate the start and stop signals for a high-precision clock timer (Tektronix DC 503A). Finallly, the pellet reaches an expansion tank with a volume of about 350 l, pumped down by three parallel turbomolecular pumps to about 10^{-7} mbar. This tank buffers the pressure increase caused by the evaporation of the pellet when it is destroyed. A plastic target is mounted inside this tank on the side opposite the exit port of the centrifuge vessel. Here, most of the pellets impact, eroding some target material. From this target plate it is possible to measure the vertical scattering angle of the pellets.

If the mass of a pellet has to be determined, part of the expansion tank can be rapidly decoupled from the rest of the system after the arrival of a pellet by a special high-speed valve (VATQUICK, switching time less than 15 ms). As the volume of this part of the tank is well known, the pellet mass can be calculated from the pressure increase measured by a calibrated THERMOVAC. To reduce gas escape during the valve closing time, a diaphragm was mounted just behind the valve. Additionally, a fine metal grid was installed to ensure rapid destruction of the pellets.

For the final mounting of the centrifuge at ASDEX Upgrade the linear detector array is integrated into the centrifuge system. A unit containing the pellet photography system can also be mounted, if necessary, to control the pellet integrity. A microwave pellet mass detector is now under development in order to allow precise determination of the mass of the pellet before it enters the plasma [13]. As the pellet velocity can be determined very percisely from the centrifuge revolution frequency, a time-of-flight measurement can be dispensed with.

3. TESTBED OPERATION RESULTS

Successful production of fuel rods is very sensitive to the temperatures and pressures applied during the processing steps; it also has to be optimized for each hydrogen isotope used. Moreover, the temperature of the storage cryostat has to be optimized in order to achieve both a high pellet-generating efficiency and a high quality of the pellets produced. If the temperature is too high, pellets become soft and get damaged more easily during the acceleration process; degeneration due to partial sublimation of the stored fuel rod may also occur during long-term storage. On the other hand, temperatures too low were found to reduce the efficiency; if the temperature is continuously decreased, fewer and fewer pellets are successfully cut from the rod. This is most probably due to freezing of the rod onto the wall of the storage cryostat, preventing the rod from being pushed by the lever. To solve this problem, a certain clearance between the fuel rod and the storage cryostat wall turned out to be helpful. The efficiency of successfully cutting a pellet from the fuel rod can then be kept much higher for temperatures a few Kelvin below the melting point. In Fig. 5 the efficiency observed for cutting a pellet from the fuel rod stored within the $(1.75\ \text{mm})^2$ channel is plotted for ice rods extruded either through the $(1.5\ \text{mm})^2$ or the $(1.75\ \text{mm})^2$ nozzle (filled and open circles, respectively). As a result of this experience, the extrusion nozzles were replaced during the testbed operation period by nozzles with widths reduced by 0.1 mm. Thus, $(1.9\ \text{mm})^2$, $(1.65\ \text{mm})^2$ or $(1.4\ \text{mm})^2$ rods are now stored within the $(2.0\ \text{mm})^2$, $(1.75\ \text{mm})^2$ or $(1.5\ \text{mm})^2$ channels.

As the temperature of the triple point is much lower for H_2 (13.9 K) than for D_2 (18.7 K) [14], the situation is much easier to handle for D_2 than for H_2. Thus, for D_2 the tolerable temperature differences are higher than those for H_2. Deuterium always shows a higher efficiency than hydrogen. With an optimized pellet production process, however, the efficiency was found to be very reproducible for each operation mode of the system; under appropriate operation conditions, often the whole fuel rod was successfully used for pellet production with all of the pellets arriving within the given acceptance angle. It was thus often possible to achieve the maximum available number of pellets from one rod (96 for 2.0 mm cubes and 128 for 1.5 mm cubes).

In order to find the appropriate centrifuge frequency range for plasma refuelling on ASDEX Upgrade, the total efficiency of pellets within the detection range of the light barrier detector array and hence within the tokamak acceptance angle was measured over the whole possible frequency range of the centrifuge. For each frequency the average was taken over about 10 fuel rods and hence about 1,000 pellets. As a typical result, efficiencies measured for H_2 pellets with a side length of 1.5 mm are shown in Fig. 6. The refuelling efficiency is found to increase with increasing centrifuge frequency, exceeding 90 % for frequencies above 60 Hz. At the two highest operation frequencies (230 and 300 Hz) almost all pellets produced are usable; for some rods already perfect output was obtained in these cases. On the other hand, a drastic decrease in efficiency results when the frequency is reduced to values below the driving pump's standby frequency of 60 Hz; fewer than half of all pellets remain within the sensitive area of the detector array at 30 Hz. This behaviour is assumed to result from repulsion of the ablating gas acting on the pellet. Whereas both the centrifugal and the compulsive forces decrease with the square of the centrifuge frequency, the repulsion forces remain at a fixed value for a given pellet species. Thus, if the frequency is decreased, repulsion forces become predominant, causing more and more disturbance of the guided acceleration of the pellet. This way,

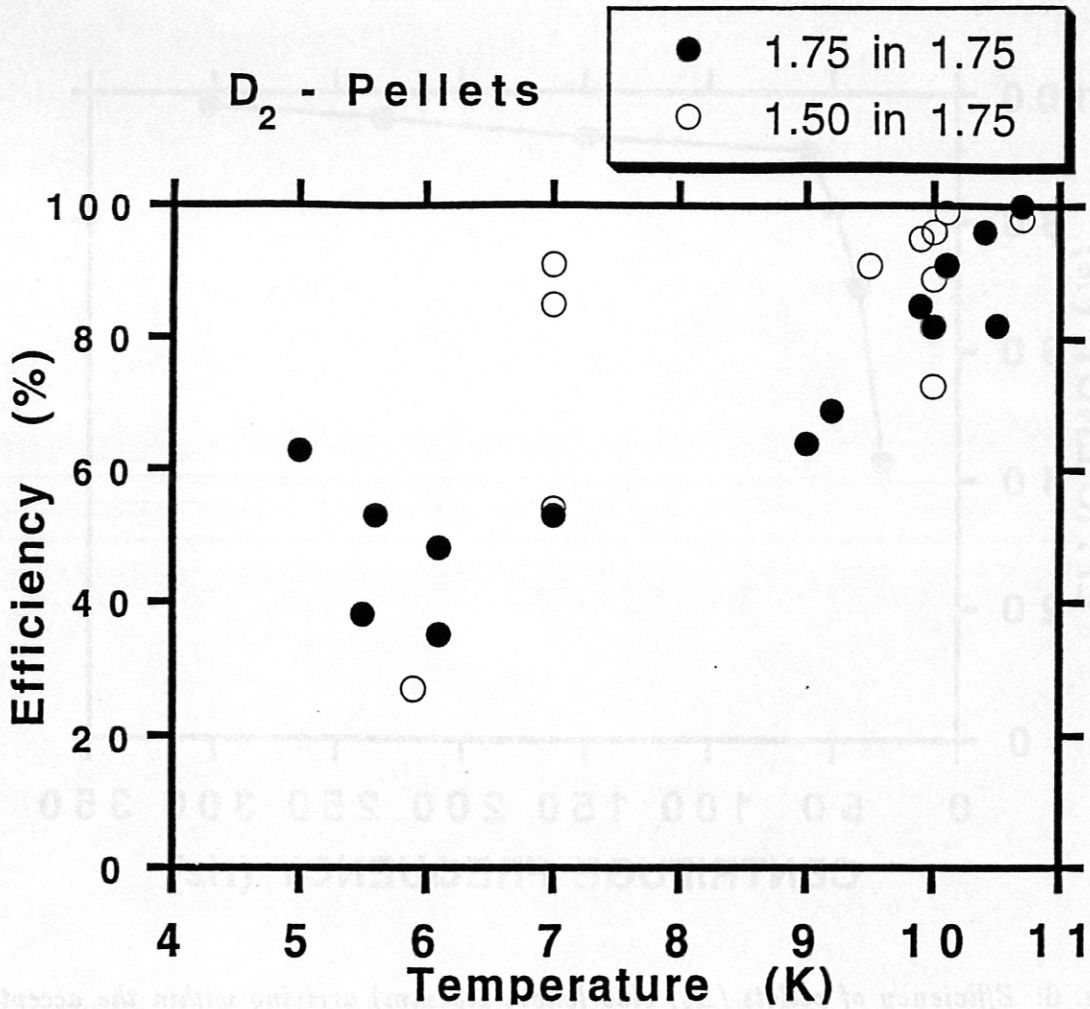

Fig. 5: *Efficiency of successfully cutting pellets from the fuel rod at different ice temperatures for a fuel rod with a square cross-section of 1.5 mm (open circles) and 1.75 mm (filled circles) extruded into the 1.75 mm channel of the storage cryostat.*

with decreasing frequency an increasing random-walk component superimposed on the nominal movement of the pellet occurs, causing the scattering angle to increase and, as a consequence, the efficiency to decrease. This belief is further supported by the results obtained from the measurements of the angular distribution of the pellets for different sizes and materials at different centrifuge frequencies. As a typical example, the angular distributions obtained for H_2 pellets of side length 1.5 mm for the frequencies 60 Hz and 300 Hz are compared in Fig. 7, showing pellets to spread over a much greater angular region for the lower frequency than for the higher one. It can also be seen from Fig. 7 that, with the stop cylinder appropriately set, the probability of pellets arriving at the edge of the acceptance angle is almost zero at f = 300 Hz, while still a lot of pellets were counted at the most outward channels for f = 60 Hz. Thus, loss of efficiency at low frequencies results from exceeding the acceptance angle. Moreover, sometimes pellets have been found to arrive at the wrong time at the detector array in the low-frequency region, again indicating an increase of perturbations with decreasing centrifugal and compulsive forces.

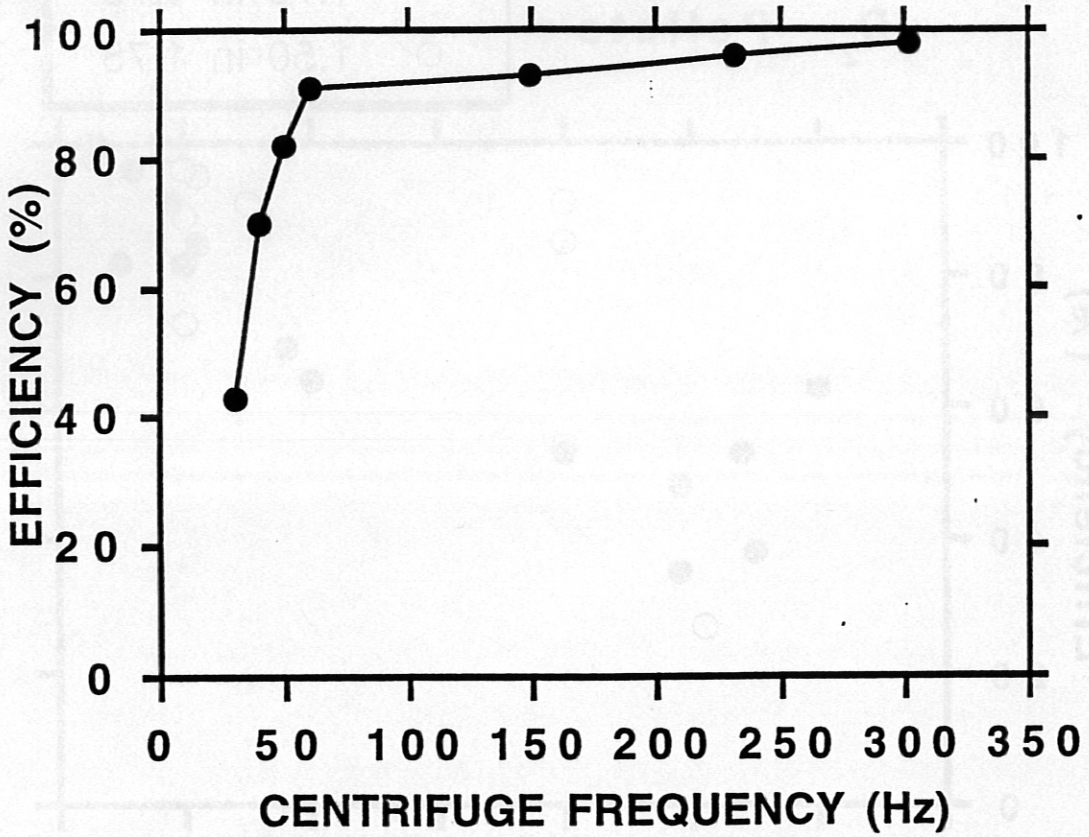

Fig. 6: *Efficiency of pellets (H_2, side length 1.5 mm) arriving within the acceptance cone valid for plasma refuelling on ASDEX Upgrade versus centrifuge frequency.*

The scattering angles for both H_2 and D_2, side lengths 1.5 and 2.0 mm and all four standard frequencies are shown in Fig. 8. From a comparison of all four pellet species it is found that the horizontal scattering angle depends only on the fuel material for low frequencies, while at high pellet velocities it is only the dimension of the cubes that is decisive. The slightly greater scattering angles of bigger pellets may result from their greater inertia affecting the exit of the pellets from the stop cylinder; the higher spatial deviations results in greater angular spread. The greater scattering angles of H_2 pellets for the lower frequencies is a further indication of ablation affecting the horizontal scattering angle, especially for low acceleration. This can easily be understood by taking into account the higher specific heat of the solid deuterium due to the higher temperature ($c_v \sim T$), the higher sublimation energy and the higher density of D_2 in relation to H_2 (H_2: 90 kg/m^3; D_2: 208 kg/m^3) [14]. This way, smaller repulsive forces act on a heavier pellet in the case of D_2, yielding less horizontal angular spread at a given frequency.

An estimate of the vertical scattering angle was made from the impact traces of the pellets on the plastic targets, showing no noticeable differences either for different pellet species or for different centrifuge frequencies. Impact traces were found to cover an area of 15 mm in height on the target mounted 3.7 m from the centrifuge, this being equivalent to a vertical scattering angle of less than ± 0.12 degree.

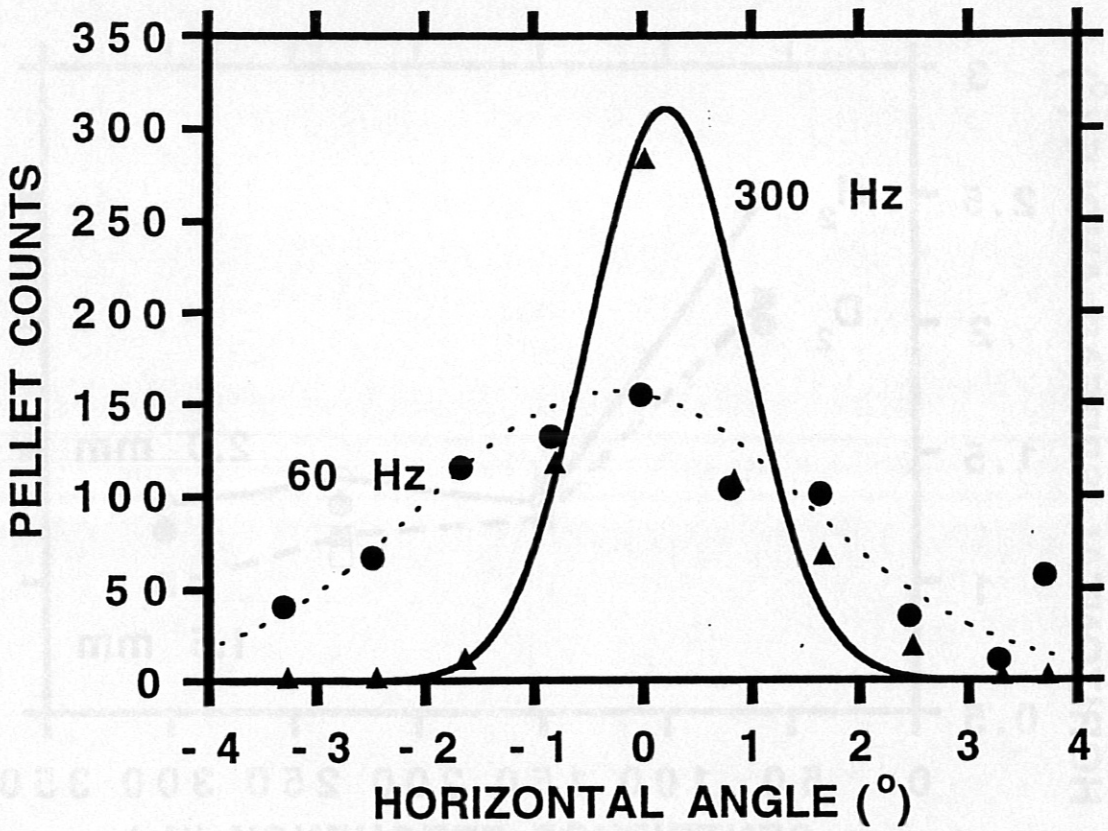

Fig. 7: *Horizontal angular distribution of H_2 pellets with a side length of 1.5 mm at centrifuge frequencies of 60 Hz and 300 Hz. Circles and triangles: count rates from the light barrier detector array; solid and dotted lines: least-squares fit to these points on the assumption of a Gaussian spatial distribution.*

The measured velocities (dots) were found to be in accordance with those calculated according to eq. 16 (solid line) within their experimental error (± 0.25 %), as shown in Fig. 9. Thus, approximations made for the calculations of the pellet velocities are permissible, especially friction being negligible for the operation range investigated.

The pellet shapes were recently measured with the CCD camera system. It was also used to control the pellet velocity further by means of the delay time between the trigger signal from the detector array and the firing of the illuminating ir laser and by means of the angular spread of the pellets, the camera system being used as a stroboscope. Conservation of the cubic shape of the pellets was found to depend sensitively on the quality of the fuel rod produced for big pellets accelerated to high velocities. In this case, some of the pellets were found to be ground down at one side or little parts of them to be split off. But even for the pellets of side length 2.0 mm accelerated to over 1200 m/s most of the pellets were found to be still undestroyed when the fuel was properly prepared. Figure 10 shows a picture of a nominal 2.0 mm deuterium pellet with $v_p = 1211$ m/s. The area of the visible square in this picture was determined to be about 2.48 × 2.67 mm, and thus the pellet was tilted with respect to the projection plane of the camera. Results similar to those for the video system were found from measurement of the pressure increase with respect to the remaining pellet mass.

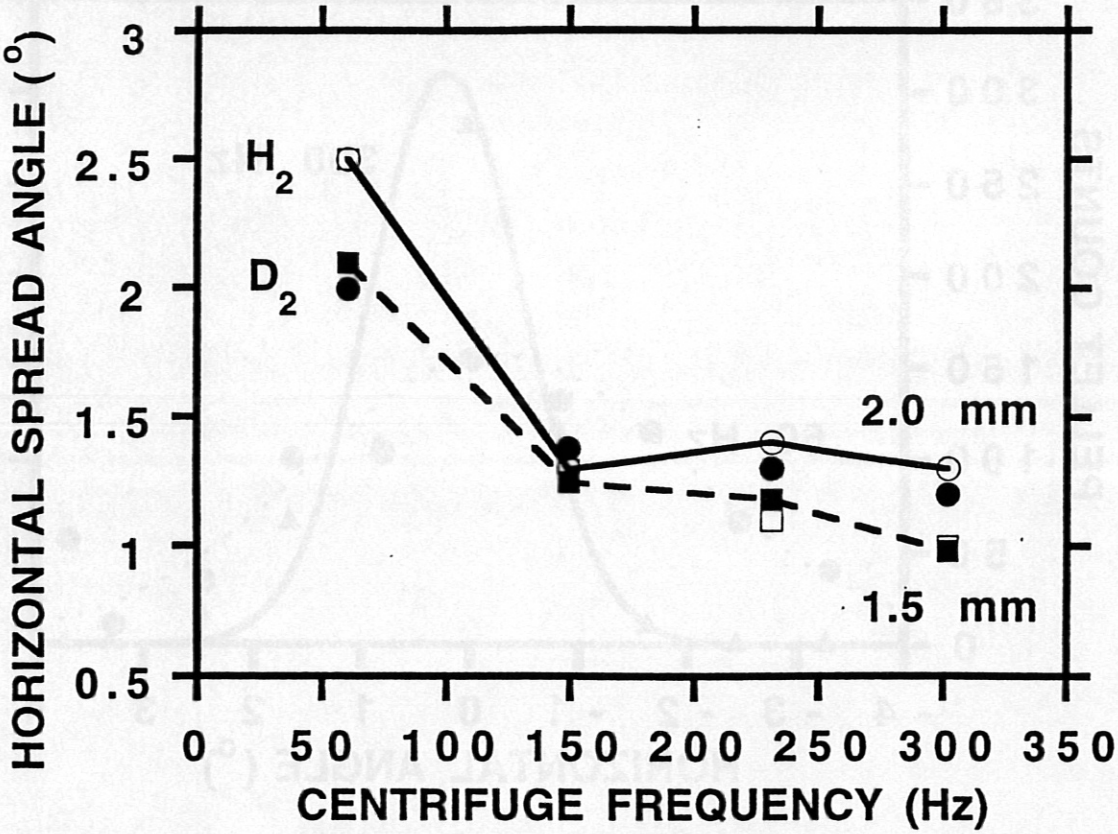

Fig. 8: *Horizontal angular spread angles (FWHM) obtained by Gaussian least-squares fits for all species of pellets. Open squares: H_2, 1.5 mm; solid line, open circles: H_2, 2.0 mm; dashed line, filled squares: D_2, 1/5 mm; filled circles: D_2, 2.0 mm.*

Again, the bigger and faster pellets are the more sensitive, in respect of their remaining mass, to the quality of the ice rod. Absolute pellet masses as calculated from the pressure increase inside the test volume measured for deuterium pellets accelerated to different velocities are plotted in Fig. 11; there, also the nominal masses of perfect pellets with the dimensions noted are indicated by broken lines. Within the experimental error of the measurement ($\approx 10 - 15$ % of the absolute value) most of the pellet species show no remarkable loss of mass. The little decrease of the measured masses in the case of a centrifuge frequency of 60 Hz is most probably due to incomplete destruction of the pellets when scattered from the vessel wall. Thus, little parts of the pellets are not yet molten at the time the pressure increase is measured ($\sim$ 3 s after injection), thus feigning a lack of pellet mass. A noticeable lack of mass, however, is indicated especially for 1.9 $mm^2\star$ 2 mm pellets at a speed of 1200 m/s (pellet mass approx. 68 % of nominal value). This was found to be due to the degradation of the fuel rod when stored at the temperature necessary for successful cutting of the pellets. If only pellets stored not more than a few minutes at temperatures near the melting point are taken into account, less loss of mass during the acceleration occurs (pellet mass approx 83 % of nominal value in this case). Thus, in order to avoid substantial loss of pellet mass during an injection experiment, the fuel rod is stored at temperatures far below the melting point and heated to appropriate temperatures for cutting the pellets from the fuel rod only a

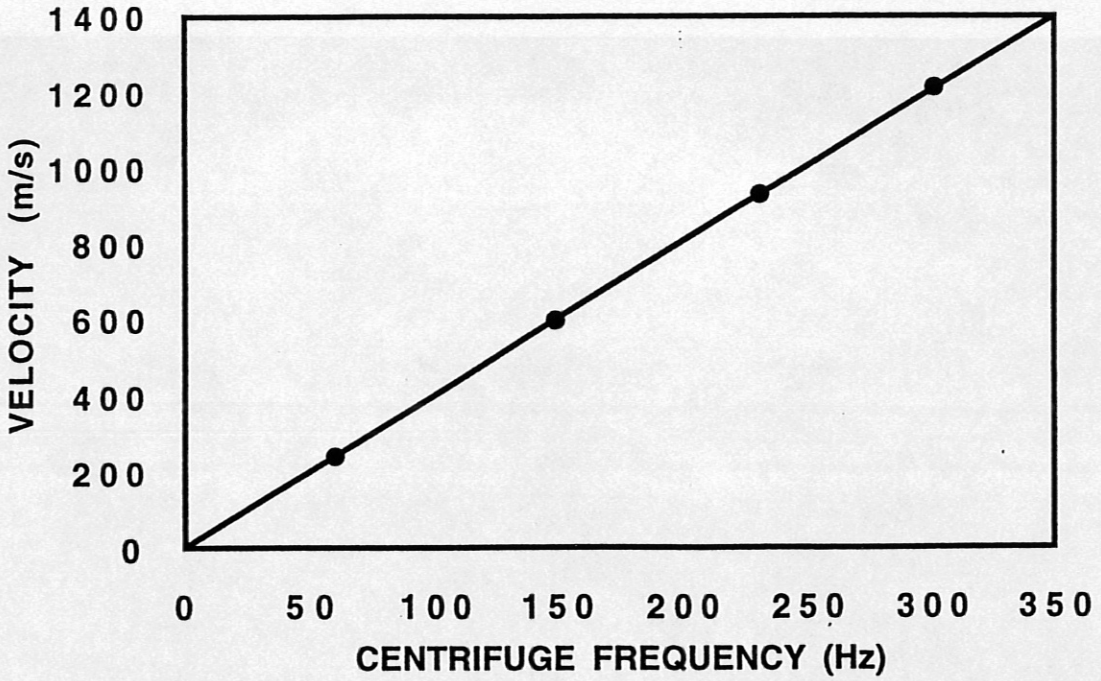

Fig. 9: *Measured pellet velocities (dots) and calculated values according to eq. (16).*

few seconds before pellet acceleration takes place. However, both the method of pellet photography and the measurement of the pressure increase inside a test volume only allows an approximate assessment of the pellet's quality since photography only yields a projection of the pellet not sensitive to any hidden holes within the pellet and the measurement of the pressure increase shows a relatively big error due to the limited closing time of the shutter valve. To achieve a more accurate diagnostics of the pellet mass and/or shapes, some further experimental effort is needed.

All results described so far were obtained from pellet sequences consisting of single pellets or series of a few pellets. This, on the one hand, conforms to the experimental requirements. On the other hand, the volume of the expansion tank was too small to prevent the pressure from increasing to values above the desired operation range in the case of larger pellet series.
In order to prove the reliability of the system, we operated it at the maximum repetition rate, injecting the whole rod at one go; thus more than 100 pellets are sucessfully injected within about 2 s.

Figures 12a and 12b show oscilloscope traces recorded during such series. Signal trace 1 indicates the stepping pulses for the lever pushing the fuel rod, there being of seven pulses each causing a 0.25 mm step, so that 1.75 mm long pellets were produced. Channel 2 recorded the signal from the photodiode mounted at the end of the storage cryostat showing the ice rod being pushed out and then cut. Signal trace 3 is a record of the 'main' trigger from the detector array, indicating the crossing of the detector by a pellet. Finally, channel 4 shows the synchronization signal from the centrifuge, this trace also showing additional signals induced by crosstalk from the electromagnetic driver of the cutter knife. In Fig. 12a the case of the minimum interval between two pellets - 23 ms at a centrifuge frequency of 300 Hz - is shown, corresponding to a maximum pellet

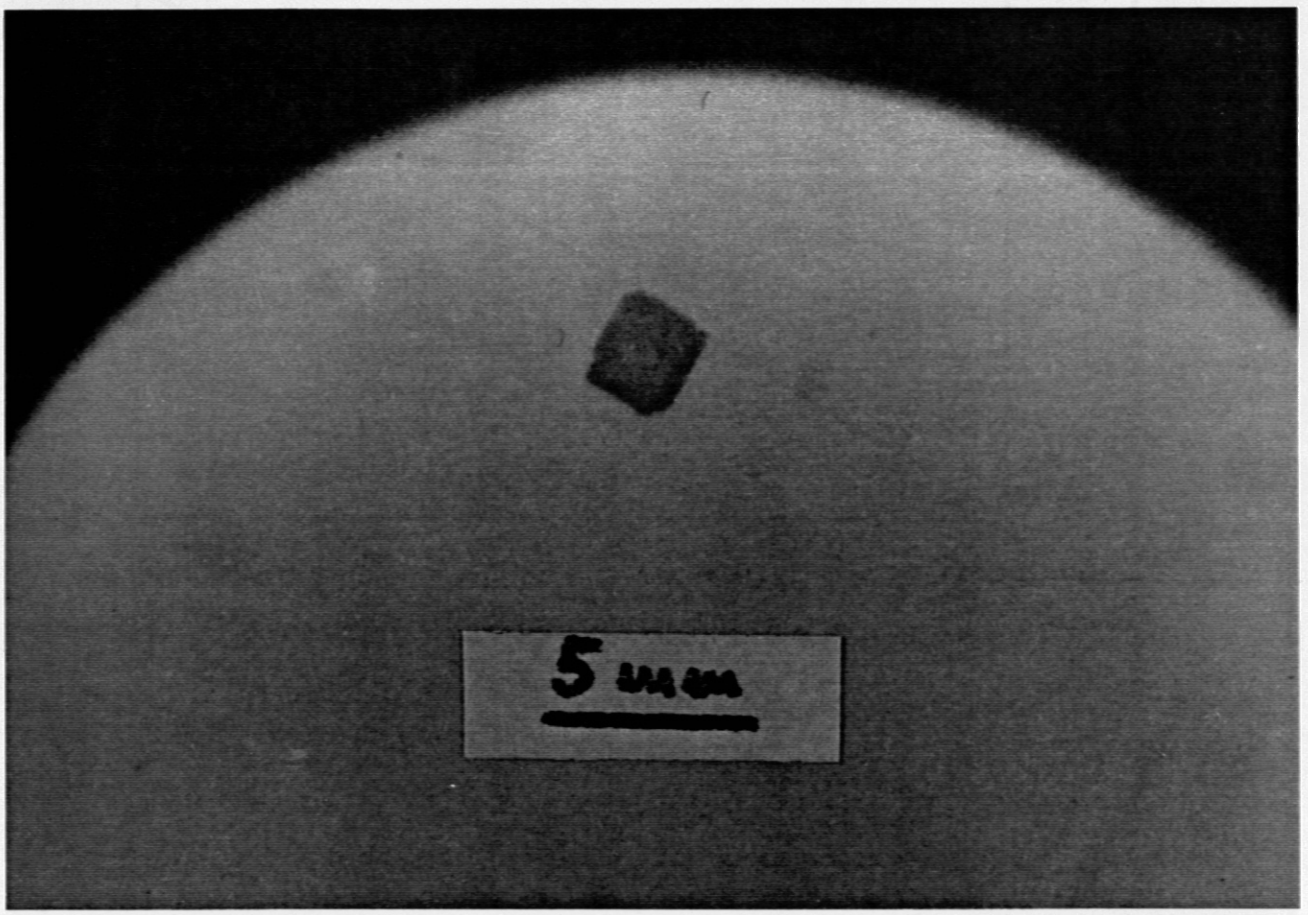

Fig. 10: *Picture of a deuterium pellet (nominal side length 2.0 mm) in flight at a velocity of 1211 m/s.*

repetition rate of 43.5 Hz. As the synchronization time can show a time jitter of one centrifuge revolution period (here 1/300 Hz = 3.33 ms) the pellet frequency can vary in the range from 38 to 43.5 Hz for $\omega = 300$ Hz. In Fig. 12b the oscilloscope trace recorded during a series of 100 pellets is shown (76 on the screen, average pellet frequency 39 Hz), demonstrating the high efficiency and reliability of the centrifuge system.

Even for such series the efficiency or the angular spread was found to be the same as that at lower pellet rates, even though the pressure operation range of the centrifuge was greatly exceeded. It should be noted that this limitation is no longer valid on a real refuelling experiment since the huge volume of current tokamaks (ASDEX Upgrade: 32.000 l) prevents such a strong increase of the pressure.
During the whole test operation period the system was found to work very reliably and reproducibly. Altogether, about 1.000 fuel rods, equivalent to 10^5 pellets, were produced.

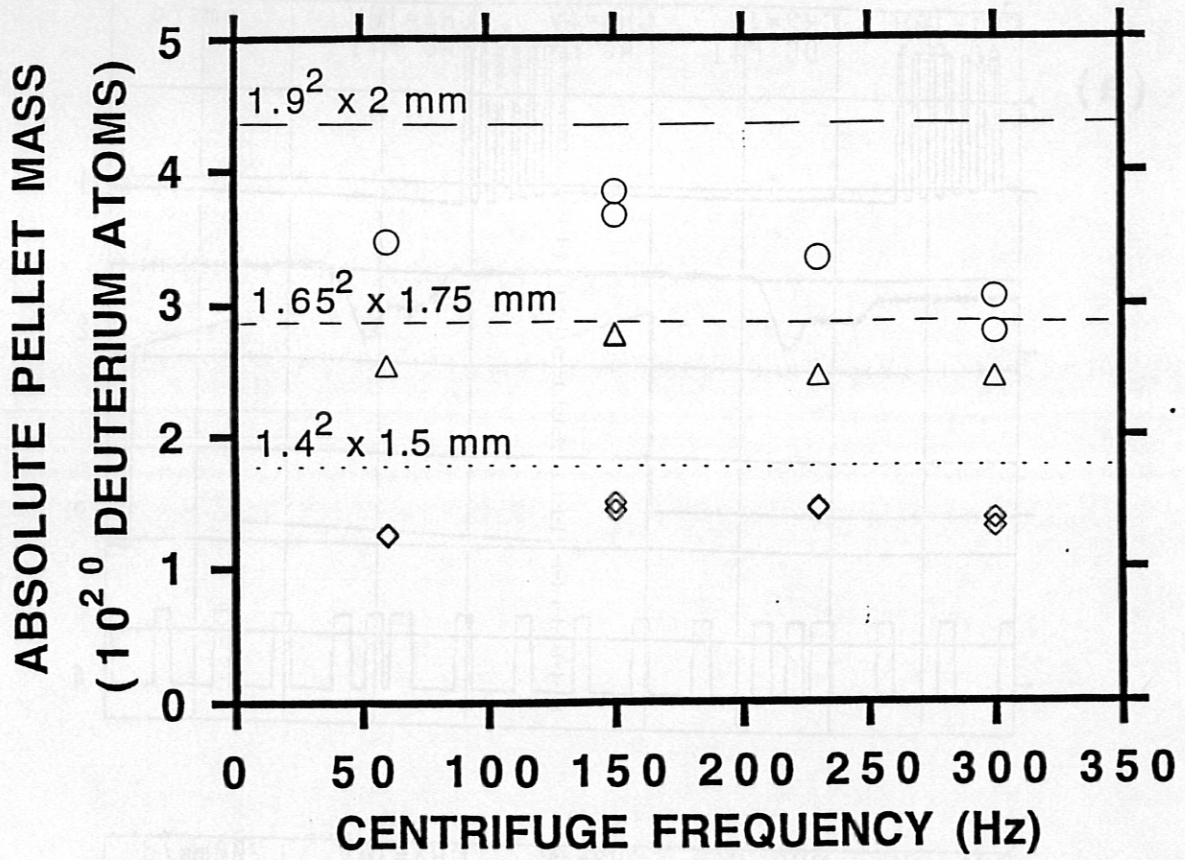

Fig. 11: *Absolute pellet masses as determined from the pressure increase within the test volume (symbols) and nominal values of the perfect pellets (broken lines, pellet dimensions indicated).*

4. CONTROL AND DATA ACQUISITION

4.1 Integration into the ASDEX Upgrade setup

The pellet centrifuge is mounted at ASDEX Upgrade in sector 5, at a distance of 5490 mm from the centre of the torus to the centre of the centrifuge. Pellets enter the tokamak via the A-port (at r = 3430 mm) at the midplane of the standard single-null plasma configuration (75 mm above the torus midplane) and 133 mm apart from the middle of sector 5 in the direction of sector 6. The mean pellet trajectory is horizontal and tilted by 11° from the radial direction towards sector 4; an opening angle of ±4° around this mean trajectory is accessible during the whole pellet injection path. For observation of the pellet ablation clouds a high-speed framing camera is also mounted in sector 5, viewing from behind the pellets and being capable of taking a picture every two microseconds. Observation of the radiation emitted in the spectral range of the Balmer-α (Hα, Dα) lines, is done with a couple of CCD cameras and a couple of photodiodes. CCD cameras are installed in sectors 5 and 6, observing the pellet from the top (ports 5E) or tangentially (6B). The photodiodes view the pellet ablation tangentially (twice in port 6B), from the top (twice in port 5E) and from behind (once in port 5A) with a time resolution of at least 2 μs. Other diagnostics systems important for the pellet injection analysis are the microwave reflectometer (sector 6) and the soft X-ray camera (sector 5),

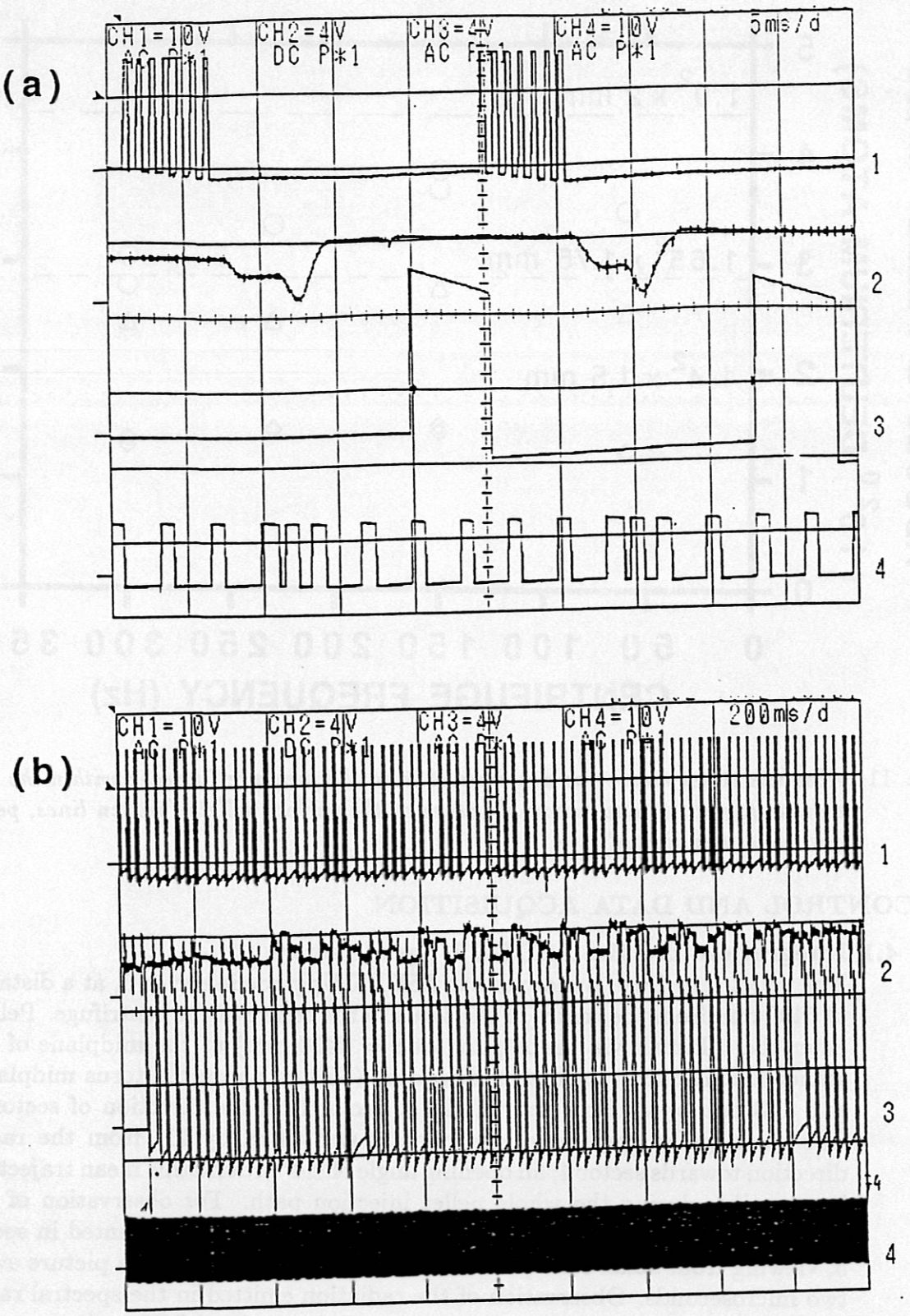

Fig. 12: *Oscilloscope traces (see text) recorded during pellet sequences of the order of 100 pellets. (a) Minimum temporal pellet distance of 23 ms; (b) high efficiency and reliability of pellet injection during a whole injection sequence.*

the Thomson and the bremsstrahlung diagnostics (sector 3), the DCN laser interferometer (sector 11) and the ECE diagnostics (sector 9). In order to allow measurement of the electron density (n_e) profile at the very same time as the pellet injection, the centrifuge system is synchronized with the Nd: YAG laser system. Therefore, centrifuge revolution frequencies had to be changed to multiples of the laser repetition frequency of 20 Hz. Thus, the centrifuge frequencies are now set to 60, 140, 220 and 300 Hz, corresponding to pellet velocities of 240, 560, 880 and 1200 m/s, respectively. An overview of the pellet parameters now available for injection into ASDEX Upgrade is given in Table I.

4.2 Operational modes of the centrifuge

The local control unit (SIMATIC "PEI") is connected to the supervisor controller (SIMATIC "SLS") by means of a SINEC H1-bus and directly coupled to the AUG valve system. Moreover, the system is equipped with a local timer and connected to the AUG safety and interlock system. The adaption of the local control unit to the master diagnostic and the safety system is given in Fig. 13. The operational mode of the centrifuge can be decided at the local control unit; there are three different modes to choose from:

- Local test: This mode is only used for internal tests of the centrifuge system. Pellets are requested locally. There is no interaction with the AUG controlling systems, the gate to the AUG entrance port being locked.

- Local shot: Upon a single-pellet request signal, usually generated by means of a local timer event, a whole sequence of pellets is injected into the tokamak. This sequence is preprogrammed and stored within the local control unit. In this mode pellet injection can be stopped by the AUG safety and interlock system.

- Central shot: This is used for quasicontinuous refuelling during a tokamak discharge by fully automatic, feedback-controlled operation of the injector. Each single pellet is injected upon a request signal arriving from the fast control unit (SSR). In this mode, pellet injection can also be interrupted by the AUG safety and interlock system.

4.3 Data acquisition and data transfer

The operational mode and possibly the pellet sequence envisaged to be injected into the tokamak are chosen and preprogrammed by the centrifuge operator before every plasma discharge. Also all pellet parameters have to be directed to the local SIEMATIC control system via the COROS shell. All the relevant data can be transferred by means of a serial V24 interface from the local control unit into the Unix system and can thus be stored within the AMOS shotfiles. Before a plasma discharge sequence starts, the volume of the pellets (in 0.01 mm^3), the pellet material (H_2 or D_2, amount of Ne admixing), the pellet velocity and, in the case of operation in the local shot mode, also the envisaged pellet sequence are transferred. After the discharge, the number of the linear detector array channel crossed by each pellet (-8, ..., 0, ..., +8) is also transferred and stored. The times at which "main" trigger pulses are delivered from the detector array are stored with a maximum temporal resolution of 2 microseconds in the Halfa diagnostics. Later on, it is scheduled to record

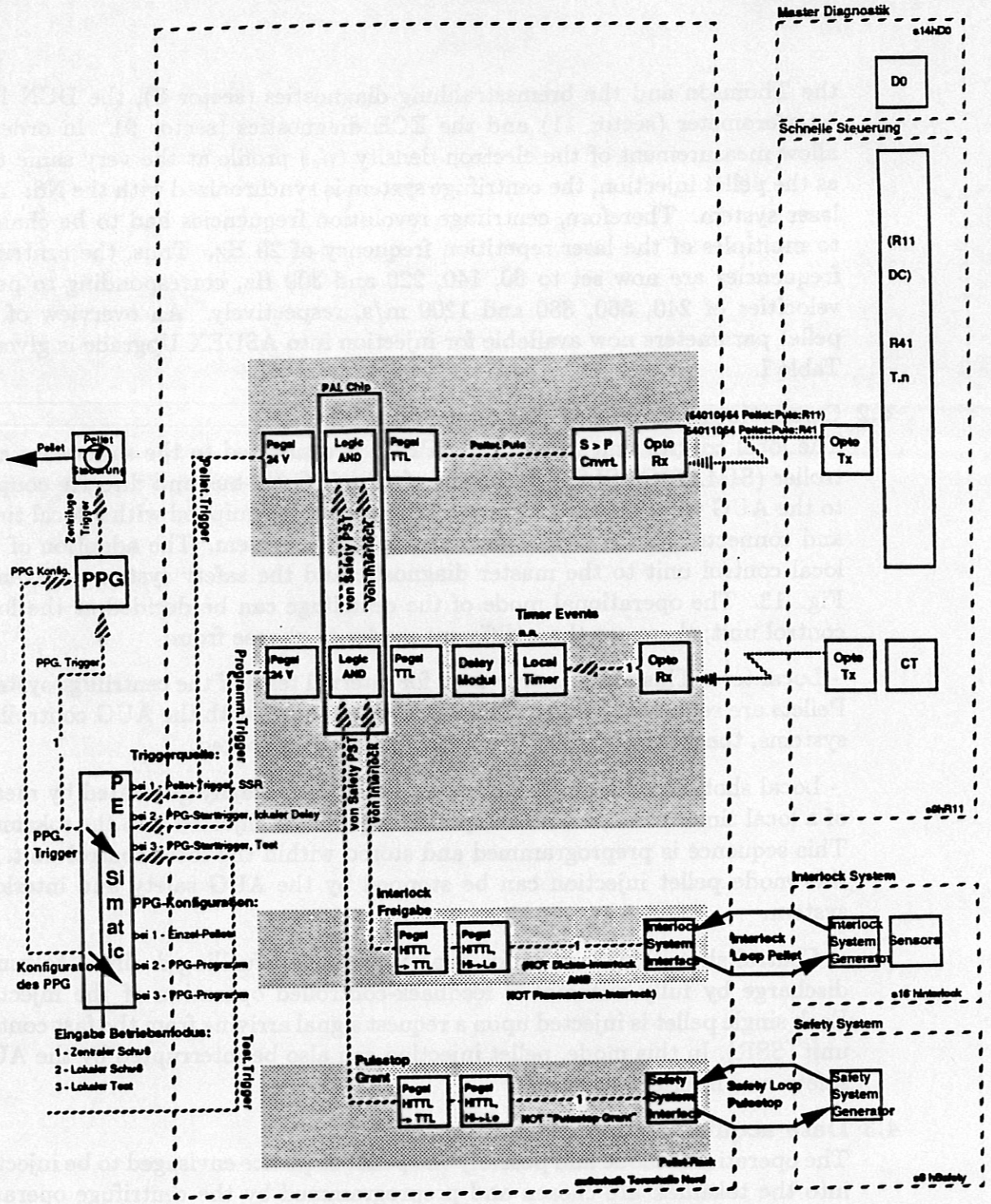

Fig. 13: *Integration of the local control unit (SIEMATIC "PEI") to the master diagnostics and the safety and interlock system.*

these events with a time resolution of 200 ns within the local timer of the centrifuge system. Thus, for each pellet injected into the tokamak the angle of the trajectory (to an accuracy better than 0.5°), the velocity (to an accuracy of 0.25 %) and the time of crossing the detector array are known, and so the flight path can be exactly reconstructed. This is necessary for further analysis.

5. SUMMARY

The centrifuge-based pellet injection system for plasma refuelling described here has been sucessfully tested and has proved to operate well and reliably for about 10^5 pellet injections so far. With this system, pellets of different sizes of both stable isotopes of hydrogen can be produced and accelerated to velocities ranging from 120 m/s to more than 1200 m/s. Pellets are available as series of up to about 130 pellets with a repetition rate of up to 43.5 Hz. As are compulsive forces minimized by using a straight acceleration arm, there is no drastic deformation of the pellets even at the highest speeds. The efficiency of the system was found to depend mainly on the horizontal spread angle of the pellets at the exit of the centrifuge. As this spread angle increases with decreasing centrifuge frequency due to the repulsion of the ablating gas acting on the pellet, most efficient operation of the centrifuge was found to occur at the highest centrifuge frequencies, a value of more than 90 % of the pellets arriving within the acceptance angle of the ASDEX Upgrade main port ($\pm 4°$) was achieved for a frequency above 60 Hz. The system described here is well suited to quasicontinuous plasma refuelling using pellets with a large mass and medium velocities both with high repetition rate and a large number of pellets. The wide range of possible pellet masses and velocities permits variation of the deposition profile over a wide range, allowing a gradual transition from central to edge fuelling

TABLE

Pellet parameters

Fuel	H_2, D_2, Ne doping optional
Cubic pellet: side length	$1.4\times1.4\times1.5, 1.65\times1.65\times1.75, 1.9\times1.9\times2.0$ mm
Pellet mass	1.7, 2.8, $4.3 \star 10^{20}$ particles
Pellets available	128, 109, 96
Pellet velocities	240, 560, 880, 1200 m/s
Velocity variation	max. 0.25%
Repetition rate	up to 43 Hz
Spread angle	
horizontal	$\sim v_p^{-0.5}, \approx 1^o$ at $v_p = 1200$ m/s
vertical	$\approx 0.1^0$
Efficiency	$> 90\%$ for $v_p > 240$ m/s $\approx 98\%$ for $v_p = 1200$ m/s

REFERENCES

[1] J. Raeder et al., Controlled Nuclear Fusion - Fundamentals of its Utilization for Energy Supply, (John Wiley & Sons, Chichester, 1986).

[2] M. Kaufmann et al., Nucl. Fusion **28**, 827 (1988).

[3] M. Kaufmann, K. Lackner, J. Neuhauser and H. Vernickel, Nucl. Fusion **25**, 89 (1985).

[4] C.T. Chang, Phys. Reports **206**, 143 (1991).

[5] K. Sonnenberg et al., Proceedings of IEEE, 12th Symposium on Fusion Engineering, Monterey CA, Oct. 12-16, 1987, Vol. 2, pp. 1207 - 1210.

[6] C.A. Foster, J. Vac. Sci. Technol. **A1**, 952 (1983).

[7] K.H. Behringer and K. Büchl, Nucl. Fusion **29**, 415 (1989).

[8] W. Amenda and R.S. Lang, J. Phys. E.: Sci. Instrum. **19**, 970 (1986).

[9] F. Scheck, Mechanik, (Springer Verlag, Berlin, 1988).

[10] W. Amenda and R.S. Lang, Refuelling of Plasma Machines by Pellet Injection with a Centrifuge, IPP Report I/187, (MPI für Plasmaphysik, Garching, Germany, March 1981).

[11] H. Neuber, Technische Mechanik, Teil 2: Elastostatik und Festigkeitslehre, (Springer Verlag, Berlin 1971).

[12] C. Andelfinger, H. Kollotzek, M. Ulrich, G. Weber and K.H. Bernhardt, Proceedings of the 11th International Vacuum Congress, Cologne, Germany, 1989, Paper S678.

[13] V. Kapralov, Mass measuring system for ASDEX Upgrade, Status seminar of the WTZ-Abkommen Pelletinjektion, St. Petersburg, January 1993.

[14] P.C. Souers, Hydrogen Properties for Fusion Energy (University of California, Berkeley Press 1986).